PSKH1 affects proliferation and invasion of osteosarcoma cells via the p38/MAPK signaling pathway

XINGFEI ZHU*, CHAO JIANG*, ZHIYUANG WANG, XIAOZHONG ZHU, FENG YUAN and YI YANG

Department of Orthopedics, Tongji Hospital, Tongji University, Shanghai 200065, P.R. China

Received September 15, 2022; Accepted February 10, 2023

DOI: 10.3892/ol.2023.13730

Abstract. Malignant osteosarcoma (OS) is a tumor of bone and soft tissue that metastasizes early and has a high mortality rate. Protein serine kinase H1 (PSKH1), an autophosphorylating human protein serine kinase, controls the trafficking of serine/arginine-rich domain, with downstream effects on mRNA processing. It is also associated with tumor progression. However, how this protein contributes to OS progression and metastasis is unknown. The present study evaluated the potential effect of PSKH1 on proliferation of human OS cells. OS cell lines were used in Cell Counting Kit-8, colony formation, wound-healing and Transwell assays, to investigate cellular processes such as proliferation, migration and invasion and underlying molecular mechanisms. Expression of PSKH1 in OS tissue was significantly greater than in adjacent non-malignant tissue. PSKH1 knockdown inhibited the proliferation, migration and invasion of OS cells. Conversely, PSKH1 overexpression promoted proliferation of OS cells. PSKH1 upregulated phosphorylated-p38 in OS cells. Moreover, the p38 MAPK inhibitor SB203580 effectively blocked the tumor-promoting action of PSKH1. Furthermore, PSKH1 knockdown inhibited tumor growth and metastasis *in vivo*. In conclusion, these findings suggested that PSKH1 promoted OS proliferation, migration and invasion. Thus, PSKH1 may serve an oncogenic role in the development of human OS.

Introduction

Osteosarcoma (OS) is the most common primary malignant bone tumor in children and adolescents; ~1,000 new cases of OS are diagnosed in the United States each year, approximately half of which are in children and teenagers. The 5-year overall survival rate is 60% (1). Post-treatment factors contributing to poor survival include incomplete surgical resection and poor response to chemotherapy (2,3). Surgery, chemotherapy and radiotherapy are currently the most common treatment options. Improvement in treatment modalities has led to a better prognosis for patients with OS but treatment efficacy remains insufficient (4,5). Therefore, better understanding of the molecular mechanism underlying OS development is key (6,7).

Protein serine kinase H1 (PSKH1) belongs to the serine/arginine-rich domain protein family with a specific localization in nuclear speckles (8,9). This gene plays an important role in the trafficking of serine/arginine-rich domains, which leads to pre-mRNA synthesis. Previous studies have demonstrated that PSKH1 plays a role in promoting cancer in humans (10,11). For example, microRNA (miR)-566 directly targets PSKH1, regulating colon cancer cell proliferation, migration and invasion (12). Various factors contribute to the development of tumors via the p38/MAPK signaling pathway (13,14). For example, downregulation of Non-SMC condensin I complex subunit G (NCAPG) could suppress OC cell proliferation and invasion via activating the p38 MAPK signaling pathway (13). The p38 pathway serves a crucial role in facilitating muscle differentiation, which confers its anti-tumor properties (15). The activation of the p38/MAPK signaling pathway leads to the reactivation of dormant disseminated tumor cells, resulting in the development of metastatic prostate cancer (16). Other studies have shown that the p38/MAPK signaling pathway promotes cancer by improving survival and migration (17,18). In early stages of cancer, low p38 activity impairs tumor formation and growth, while a higher level of activation of the p38/MAPK pathway contributes to survival and proliferation of tumor cells for more advanced tumor stages (19). In late stages of tumorigenesis, p38 inhibits cancer cell migration to neighboring tissue (20). Nuclear antigen Ki-67 is only found in proliferating cells (21) at the G1, S, and G2 phases of the cell cycle and mitosis, but is absent from resting cells at G0 (22). In cancer cells, it is widely used as a proliferation marker (23-25). It has been found that Ki-67 is associated with tumor metastasis in several studies (26,27). Zeng *et al* (28) reported that positive Ki-67 expression is associated with distant metastasis and overall survival of OS. However, the biological role of PSKH1 in OS cells and the association between PSKH1, p38/MAPK signaling pathway and Ki-67 expression remain unclear.

Correspondence to: Dr Yi Yang, Department of Orthopedics, Tongji Hospital, Tongji University, 389 Xincun Road, Shanghai 200065, P.R. China
E-mail: yangyi1987@tongji.edu.cn

*Contributed equally

Key words: osteosarcoma, protein serine kinase H1, cell proliferation, cell invasion, p38, therapeutic target

The present study aimed to explore the role and underlying molecular mechanism of PSKH1 in OS cells.

Materials and methods

Bioinformatics analysis. Gene expression profiles of 37 OS cases were obtained from the Gene Expression Omnibus (GEO, ncbi.nlm.nih.gov/geo/) database (accession no. GSE 39055). Expression profiling was performed using an Illumina HumanHT-12 WG-DASL V4.0 R2 Expression BeadChip (Illumina, Inc.). All mRNA expression datasets were retrieved from the GEO database. Analysis of differentially expressed mRNAs of tumor tissue was performed using the DESeq2 package in R (version 1.20.0) (29). Samples were stratified based on the mean expression levels of PSKH1. Survival and ggplot2 packages in R were used for survival analysis and plotting.

Gene set enrichment analysis (GSEA). GSEA was used to identify potential biological pathways and processes associated with PSKH1. mRNA expression data were obtained from ArrayExpress (https://www.ebi.ac.uk/biostudies/arrayexpress) (accession no. E-MEXP-3628), including four normal bone and 14 OS tissue samples. The dataset was extracted from the Molecular Signatures Database on the GSEA website (gsea-msigdb.org/gsea/index.jsp). Next, A weighted enrichment analysis was carried out utilizing the GSEA 2.2.2 software, which involved the selection of 1,000 random combinations (30).

RNA extraction and reverse transcription-quantitative (RT-q) PCR. Total SAOS2, HOS, MG63 and U2OS and osteoblastic hFOB1.19 cells or transfected SAOS2, U2OS and MG63 cells RNA was isolated using TRIzol reagent (Invitrogen; Thermo Fisher Scientific, Inc.). RNA was dissolved in 0.025 ml nuclease-free water and stored at -80˚C. cDNA synthesis was performed using the SuperScript First-Strand Synthesis System (Thermo Fisher Scientific, Inc.) according to the manufacturer's instructions. Thermocycling was performed at 95˚C for 10 min, followed by 40 cycles at 95˚C for 15 sec and 60˚C for 45 sec. qPCR was then performed using SYBR Green PCR Master Mix (Thermo Fisher Scientific, Inc.), according to the manufacturer's protocol. PCR amplification was performed in triplicate. Primers were as follows: PSKH1: Forward, 5'-GCT GTGGGACAAGCAAGG-3' and reverse, 5'-TGGTGGTTC TGAGGGAGG-3' and β-actin: Forward, 5'-AATGAGCGG TTCCGTTGC-3' and reverse, 5'-TCTTCATGGTGCTGG GAG-3'. β-actin was used as an internal reference to calculate the relative expression of PSKH1. Relative gene expression was analyzed using 2-ΔΔCq method (31).

Western blotting. The SAOS2, HOS, MG63 and U2OS and osteoblastic hFOB1.19 cells or transfected SAOS2, U2OS and MG63 cells lysate was prepared using ice-cold RIPA lysis buffer (Beyotime Institute of Biotechnology). BCA Protein Assay kit was used to determine the concentration of protein. Whole cell lysate (25 μg/lane) was electrophoresed on 10% sodium dodecyl sulfate-polyacrylamide gel and semi-dry transferred onto polyvinylidene difluoride membranes. Membranes were blocked with 5% skimmed milk in Tris-buffered saline with 0.5% Tween-20 (TBST) for 1 h at room temperature, then incubated overnight at 4˚C with primary antibodies in TBST containing 5% skimmed milk. Primary antibodies were as follows: PSKH1 (1:500, cat. no. Sc-514401, Santa Cruz Biotechnology, Inc.), p38 (1:2,000, cat. no. Ab170099, Abcam), phosphorylated (p)-p38 (1:1,000; cat. no. Ab47363, Abcam) and β-actin (1:5,000; cat. no. 66009-1-lg, Proteintech Group, Inc.). Membranes were washed and incubated at room temperature for 30 min with horseradish peroxidase-conjugated with goat anti-rabbit (1:1,000; cat. no. A0208, Shanghai Biyuntian Bio-Technology Co. Ltd.) and anti-mouse secondary antibodies (1:1,000; cat. no. A0216, Shanghai Biyuntian Bio-Technology Co. Ltd.). Membranes were washed three times with TBST and bound proteins were visualized using Immobilon chemiluminescent HRP substrate (Millipore,Sigma) and detected using BioImaging Systems (Tanon Science and Technology Co., Ltd.). β-actin was used as an internal control to verify basal protein expression levels using Image Lab software (version 6.0; Bio-Rad Laboratories, Inc.).

Cell culture. Human OS SAOS2, HOS, MG63 and U2OS and osteoblastic hFOB1.19 cell lines were purchased from the American Type Culture Collection (ATCC). Standard protocols for cell culture were followed (32). SAOS2, HOS and MG63 cells were cultured in a Minimum Essential Medium (Hyclone) supplemented with 10% fetal bovine serum (FBS) (Gibco) and 1% penicillin/streptomycin (Beijing Solarbio Science & Technology Co., Ltd.). U2OS and hFOB1.19 cells were cultured in RPMI-1640 (Hyclone) supplemented with 10% FBS and 1% penicillin/streptomycin (Beijing Solarbio Science & Technology Co., Ltd.). Cells were incubated at 37˚C in a humidified incubator with 5% CO_2. In rescue experiments, cells were pretreated with p38/MAPK inhibitor SB203580 (cat. no. ab120162; Abcam) or DMSO for 1 h at 37˚C.

Construction of lentivirus and cell transfection. For the knockdown of PSKH1, human short hairpin (sh) RNA sequences (shRNA-1, 5'-CCGGTCCCAGCAGCA AGTCAGTATCTCGAGATACTGACTTGCTGCTGG TGTTTTG-3', shRNA-2, 5'-CCGGTGCTCTTTGACCGCA TCATTCTCGAGAATGATGCGGTCAAAGAGCTTTTTG-3' and shRNA-3, 5'-CCGGTCCTGAGAATCTGCTCTACT CTCGAGAGTAGAGCAGATTCTCAGGTTTTTG-3') and negative control (NC) shRNA (5'-CCGGTGTTCAGTGC CTACACGATTCTCGAGAATCGTGTAGGCACTGAACT TTTTG-3') were synthesized by Genewiz, Inc. at the final concentration of 1 μg/μl and cloned into the PLKO.1 plasmid (Addgene, Inc.) to generate PLKO.1-shPSKH1. The transfection of 293T cells (at 90% confluence) with a combination of PLKO.1-shPSKH1 (1,000 ng), psPAX2 (900 ng), and pMD2G (100 ng; both Addgene, Inc.) was performed utilizing the 2nd generation system and Lipofectamine 2000 (by Invitrogen, Thermo Fisher Scientific, Inc.) following the manufacturer's protocols.293T cells were obtained from ATCC. Transfection was performed for 4 h at 37˚C, then DMEM (Gibco) was replaced with complete medium for 72 h at 37˚C. The supernatant of 293T cells was collected, centrifuged at 4,000 x g for 10 min at 4˚C to remove cell debris, filtered, centrifuged at 7,000 x g for 5 min at 4˚C and resuspended in ice-cold PBS to detect the titer. The infectious titer was determined by

hole-by-dilution titer assay. The quantity of lentiviral plasmid used for transfection was 5 μg. Cells were divided into PSKH1 knockdown (LvshPSKH1) and NC groups. The SAOS2 and U2OS cells at a density of $5x10^4$ cells/well in a 6-well culture plate were infected with LvshPSKH1 or shNC with a multiplicity of infection of 20. After 48 h transfection at 37˚C, the selection of stable cell lines was performed with puromycin (Sigma-Aldrich, Merck KGaA) at 4 μg/ml for 2 weeks. The concentration of puromycin used for maintenance was 1 μg/ml. SAOS2 and U2OS cells were used in further experiments.

In addition, human PSKH1 mRNA sequences were synthesized by Genewiz, Inc. and cloned into the pLVX-Puro vector (Clontech; Takara Bio USA) to generate pLVX-Puro-PSKH1 Plasmids. All constructs were verified by DNA sequencing. A 2nd generation system was used to package the lentivirus. A total of 1,000 ng constructed plasmids together with packaging (100 ng psPAX2) and envelope plasmid (900 ng pMD2G; both Addgene, Inc.) was transfected for 4 h at room temperature using Lipofectamine 2000 (Invitrogen; Thermo Fisher Scientific, Inc.) in 293T cells (90% confluency) according to the manufacturer's instructions. DMEM was replaced with full culture medium for 48 h at 37˚C. The supernatant of 293T cells was collected, centrifuged at 4,000 x g for 10 min at 4˚C to remove cell debris, filtered, centrifuged at 7,000 x g for 5 min at 4˚C and resuspended in ice-cold PBS to detect the titer. The infectious titer was determined by hole-by-dilution titer assay. The quantity of lentiviral plasmid used for transfection was 5 μg. Cells were divided into PSKH1 overexpression (oePSKH1) and vector groups. MG63 cells at a density of $5x10^4$ cells/well in a 6-well culture plate were infected with oePSKH1 with a multiplicity of infection of 5. After 48 h transfection at 37˚C,stable cell lines were selected by puromycin (Sigma-Aldrich; Merck KGaA) at 4 μg/ml for 2 weeks. The concentration of puromycin used for maintenance was 1 μg/ml. The cells were used for downstream assay or transplantation.

Cell proliferation assay. Cell Counting Kit-8 (SAB Biotech; cat. no. CP002) was used to measure cell proliferation. A total of ~$3x10^4$ transfected SAOS2, U2OS and MG63 cells/well was seeded in 96-well plates and cultured overnight at 37˚C. A total of ~10 ml CCK-8 solution was mixed with 100 ml medium and added to each well. Samples were incubated for 1 h at 37˚C. The optical density was measured at 450 nm using a microplate reader (Perlong Medical Equipment Co., Ltd.).

Cell cycle analysis. Stable transfected SAOS2, U2OS and MG63 cells were washed twice with ice-cold PBS and fixed with ice-cold 70% ethanol overnight at 4˚C, cells were harvested by centrifugation at 1,000 x g for 5 min at room temperature and resuspended in PBS. Cells were stained with 0.5 ml staining buffer, 25 μl propidium iodide and 10 μl RNase A at 37˚C for 30 min in the dark. Cell cycle were detected using FACS Caliber flow cytometer (Beckman Coulter, Inc.) The results were analyzed using FlowJo software (version 10.6.2; BD Biosciences) to determine cell cycle phase.

Wound healing assay. A wound assay was employed to evaluate cell migration, as previously described (33), Stable transfected SAOS2, U2OS and MG63 cells ($5x10^5$/well) were seeded in 12-well plates and grown to nearly 100% confluence in 10% FBS-containing medium, before being washed with PBS and transferred to serum-free medium overnight at 37˚C. A 100-microliter pipette tip was used to create an artificial wound through the monolayer. After washing three times with PBS, the wound size was measured after 0, 12 and 24 h. Wound areas were photographed under an inverted fluorescence microscope (XDS-500C, Cai Kang Optical Instrument Co., Ltd., Shanghai, China) with a magnification of x40. The area of wound closure was quantified using ImageJ software (v1.8.0; National Institutes of Health).

Transwell assay. Matrigel (BD Biosciences) and Transwell chambers with 8-μm pores (Corning, Inc.) were used for Transwell invasion assay. Defrosted Matrigel glue at 4˚C was diluted in MEM (Hyclone) at a 1:2 ratio. In the upper chamber, 80 μl diluted Matrigel glue was used for the invasion assay at 37˚C for 30 min. Transwell chambers were placed in 24-well plates. The lower chamber was filled with 800 μl MEM containing 10% FBS. The upper chamber was filled with 200 μl serum-free medium and $2x10^4$ transfected SAOS2, U2OS and MG63 cells per well were seeded for 24 h at 37˚C. A total of 1 ml 0.5% crystal violet solution was added to each well. After 30 min at room temperature, each well was washed three times with 1X PBS. Cells in five randomly selected areas under the light microscope (20x magnification) were counted (CX41RF, Olympus).

Colony formation assay. Stable transfected SAOS2, U2OS and MG63 cells were seeded in 96-well-plates at 1,000 cells/well and cultivated at 37˚C for 21 days until clones (>10 cells) could be seen with the naked eye. Cells were fixed with 100% methanol and incubated for 15 min at room temperature. 0.5% Crystal violet staining was used for 30 min at room temperature to visualize the cells. Each sample was tested in triplicate. The cell clones were counted with the naked eye. The clone formation rate was calculated as follows: (Number of clones/number of inoculated cells) x100.

Xenografts in athymic nude mice. A total of 40 nude female BALB/c mice (age, 4-6 weeks; weight, 18-20 g) were obtained from Silaike Experimental Animal Limited Liability Company (Shanghai, China). Mice were maintained in a pathogen-free facility at Tongji Hospital with each cage containing 4-5 mice. Mice were maintained under standard 12/12-h light/dark conditions with food and water *ad libitum*. They were kept in a controlled environment with regulated temperature (22-24˚C) and humidity (65-70%). The present study was approved by the Ethics Committee for Animal Experiments of Tongji Hospital. Animals were handled according to The Guide for the Care and Use of Laboratory Animals (34). All mice were euthanized at the end of the experiment. The total duration of the experiment was 5 weeks. No mice died prematurely during the experiment. Mice were subjected to 4% isoflurane for inhalant anesthesia induction and 1.5% for maintenance. The mice were subcutaneously injected with $5x10^6$ U2OS cells in the armpits of nude mice. A total of 16 mice were randomly distributed into shNC (mice injected subcutaneously with U2OS cells transduced with shNC) and shPSKH1 groups

(mice injected subcutaneously with U2OS cells transduced with shPSKH1) (n=8/group). Measurements of tumor length and width were taken weekly. Tumor volume was calculated as follows: Tumor volume=(Length x width^2)/2. After 33 days, mice were anesthetized with 4% isoflurane, sacrificed by cervical dislocation and death was confirmed by breathing cessation. Tumors were dissected, weighed and fixed in 10% formalin overnight at 4˚C. No animals reached the humane endpoints, as follows: Total tumor volume of 1,500 mm^3, 15% loss of body weight, vomiting or inability to stand to reach food and water.

Hematoxylin and eosin (HE) staining. HE staining was performed according to standard protocols (35). The tumor tissue was excised and fixed in 10% formalin for 24 h at 4˚C. After alcohol gradient dehydration, ~6-μm-thick coronal sections were embedded in transparent paraffin, and dewaxing was performed with xylene. Each tissue section was incubated at 62˚C for 30 min. A series of descending ethanol (100, 90, 80 and 70%) was used to dehydrate samples for 5-10 min and samples were rinsed with distilled water for 10 min. The tissue section was subjected to hematoxylin staining and differentiated using 1% hydrochloric acid alcohol to reduce nonspecific background staining and enhance visual contrast. The tissue was rinsed with water, followed by counterstaining with 5% eosin. The slide was subsequently dehydrated using sequential washes with 80, 95, and 100% alcohol and finally cleared with xylene. The sections were sealed with neutral resin and placed in an oven at 65˚C for 15 min. These slides were observed optical microscope (Nikon Corporation) at x200 magnification.

Immunofluorescence (IF) staining. The tumor tissue was excised and fixed in 10% formalin for 24 h at 4˚C. Paraffin-embedded tissue samples were cut into 5-μm-thick sections for IHC. Sections were deparaffinized in xylene and rehydrated through graded alcohol series to water. Sections were rinsed for 10 min in distilled water, and antigen retrieval was performed by autoclaving the sections in 0.01 M citrate buffer (pH 6.0) for 15 min at 121˚C. After washing with PBS, non-specific protein binding was prevented by incubating the sample with 5% skimmed milk at room temperature for 30 min. The primary antibody for E Cadherin (cat. no. ab231303; Abcam), Ki-67 (cat. no. ab16667; Abcam) was diluted at 1:100 in a humidified container and incubated overnight at 4˚C. Following three washes in PBS, slides were incubated with Alexa Fluor 488-conjugated goat anti-mouse IgG secondary antibodies (dilution1:100, cat. no. A0428) and anti-rabbit IgG secondary antibodies (dilution1:100, cat.no. A0423,both Beyotime Institute of Technology) for 1 h at room temperature. The nuclei were counterstained with 4',6-diamidino-2-phenylindole (DAPI). All sections were photographed on a Nikon Eclipse fluorescence microscope (Nikon Corporation) at x400 magnification.

Experimental metastasis model. BALB/c nude mice were injected in the tail vein with 1x10^7 U2OS cells. Animals were randomly distributed into shNC and shPSKH1 groups (n=12/group). All animals were euthanized after 8 weeks. Metastatic nodules in the lungs were counted manually and photographed.

Statistical analysis. All data are expressed as the mean ± SD. For comparisons between multiple groups, one-way ANOVA followed by Tukey's post hoc test was conducted using GraphPad Prism (GraphPad Prism 8; GraphPad Software, Inc.). Additionally, log-rank test was used to compare Kaplan-Meier survival curves. $P<0.05$ was considered to indicate a statistically significant difference.

Results

High PSKH1 expression is associated with poor survival in patients with OS. To determine the promotive or suppressive effect of PSKH1 on overall survival of patients, PSKH1 expression was evaluated in OS and normal tissue based on the ArrayExpress database. Expression levels of PSKH1 were significantly higher in OS compared with normal bone tissue (Fig. 1A). PSKH1 expression was negatively associated with overall and recurrence-free survival of patients with OS (Fig. 1B and C). Collectively, these data indicated that high PSKH1 expression independently predicted poor survival for patients with OS.

Role of PSKH1 in OS cell lines. To understand how PSKH1 contributes to OS development, PSKH1 expression levels were detected in OS cell lines using RT-qPCR and western blotting with human osteoblast hFOB1.19 cells as control. The results showed upregulation of PSKH1 mRNA and protein in OS cells (Fig. 1D and E). These results suggest that PSKH1 may be involved in the development of OS.

MG63 cells with relatively low expression of PSKH1 were infected with PSKH1 lentivirus or control virus and a stable PSKH1 overexpressing cell line was successfully generated (Fig. 2A and B). PSKH1 was successfully knocked down in U2OS and SAOS2 cell lines by infecting cells with lenti-shPSKH1 and lenti-sh-control virus (Fig. 2C-F).

PSKH1 knockdown inhibits OS cell migration and proliferation in vitro. Knockdown of PSKH1 inhibited migration of U2OS and SAOS2 cells (Fig. 3A). The role of PSKH1 in tumorigenesis was investigated using CCK-8 and colony formation assays. Silencing PSKH1 expression significantly decreased proliferation of U2OS and SAOS2 cells (Fig. 4A), whereas cell migration and proliferation were significantly increased in MG63 cells infected with PSKH1 lentivirus compared with NC (Fig. 5A and C). Silencing of PSKH1 by shPSKH1 decreased the colony number of U2OS and SAOS2 cells (Fig. 3B), whereas PSKH1 overexpression yielded the opposite result (Fig. 5B). Together, these results suggested that PSKH1 knockdown inhibited OS cell migration and proliferation.

PSKH1 knockdown in OS cells inhibits invasion and cell cycle transition in vitro. Transwell assay was performed to verify the effect of PSKH1 on the invasion of OS cells. Silencing PSKH1 expression decreased the number of invaded OS cells (Fig. 4B). However, PSKH1 overexpression showed the opposite effect (Fig. 5D). The effect of PSKH1 on the cell cycle of OS cells was investigated. Compared with the empty vector group, silencing of PSKH1 led to a significant increase in the number of cells in the G1 phase, accompanied by a decrease

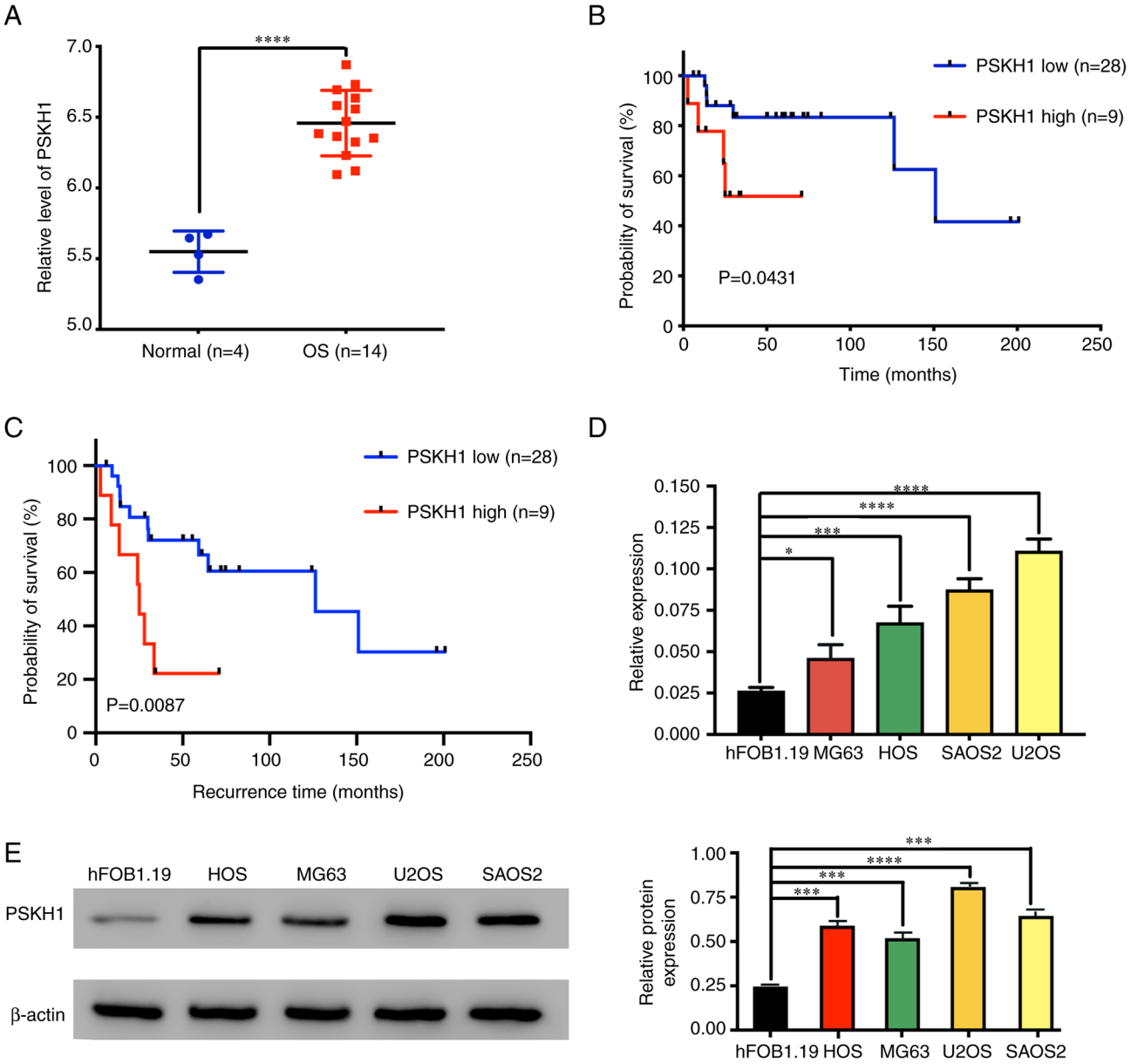

Figure 1. PSKH1 overexpression in OS tissue and human OS cells is associated with worse prognosis. (A) Expression of PSKH1 in OS and normal tissue in the ArrayExpress database (****P<0.0001 vs. Normal). (B) Kaplan-Meier curve of overall survival stratified by PSKH1 levels using the GSE39055 dataset. The cutoff value for high and low PSKH1 expression was the mean value of PSKH1. (C) Kaplan-Meier curve of relapse-free survival stratified by PSKH1 levels using the GSE39055 dataset. PSKH1 (D) mRNA and (E) protein in a panel of hFOB1.19 osteoblast cells and human OS cell lines, as detected by quantitative PCR and western blot analysis. β-actin served as an internal control. OS, osteosarcoma; PSKH1, protein serine kinase H1 (*P<0.05; ***P<0.001; ****P<0.0001 vs. hFOB1.19 osteoblast cells).

in the proportion of cells in the S and G2 phase (Fig. 4C). Overexpression of PSKH1 was found to decrease the number of cells in G1 phase, with a corresponding increase in the proportion of cells in the S phase (Fig. 5E). PSKH1 expression levels were positively associated with OS cell proliferation, invasion and cell cycle progression.

PSKH1 downregulation inhibits tumor growth in vivo. The effect of PSKH1 on proliferation of OS cells was assessed using a mouse xenograft model. PSKH1 knockdown notably inhibited tumor growth (Fig. 6A). Immunofluorescence analysis revealed that Ki67 expression was decreased in shPSKH1 group (Fig. 6B). PSKH1 knockdown tumors had significantly smaller volume and weight than control tumors (P<0.01; Fig. 6C), indicating that expression of PSKH1 promoted tumor growth in solid tumors. Overall, these results suggested that PSKH1 knockdown inhibited OS tumor growth *in vivo*.

PSKH1 knockdown suppresses pulmonary metastasis in vivo. A lung metastasis mouse model was also established by injecting shNC- and shPSKH1-U2OS cells into the tail veins of nude mice. Mice were then sacrificed 8 weeks after injection to examine metastatic nodes in the lung. E-cadherin expression was significantly decreased in the shPSKH1 group (Fig. 6D and E). PSKH1 decreased the number of metastatic tumor nodes in mice. Collectively, these results indicated that PSKH1 downregulation inhibited lung metastasis.

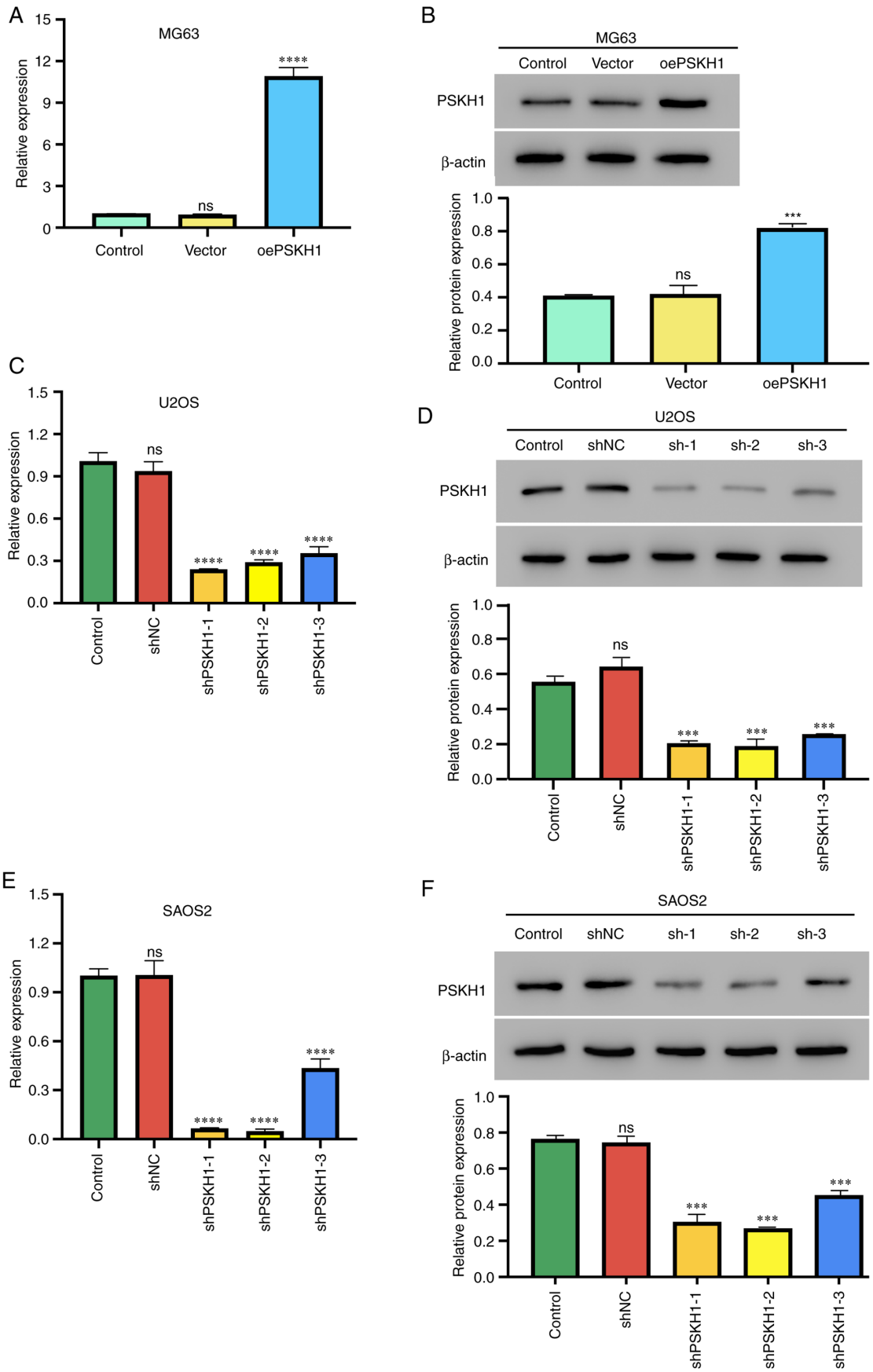

Figure 2. PSKH1 was stably overexpressed and silenced in human OS cells by transfection and selection. (A) The expression level of PSKH1 is detected by qRT-PCR in MG63 cells after PSKH1 was overexpressed. (B) The protein expression of PSKH1 is detected by Western-blot in MG63 cells after PSKH1 was overexpressed. (C) The expression level of PSKH1 is detected by qRT-PCR in U2OS cells after PSKH1 was silenced. (D) The protein expression of PSKH1 is detected by Western-blot in U2OS cells after PSKH1was silenced. (E) The expression level of PSKH1 is detected by qRT-PCR in SAOS2 cells after PSKH1 was silenced. (F) The protein expression of PSKH1 is detected by Western-blot in SAOS2 cells after PSKH1 was silenced. PSKH1, protein serine kinase H1; oe, overexpression; sh, short hairpin; NC, negative control (***P<0.001; ****P<0.0001 vs. Control).

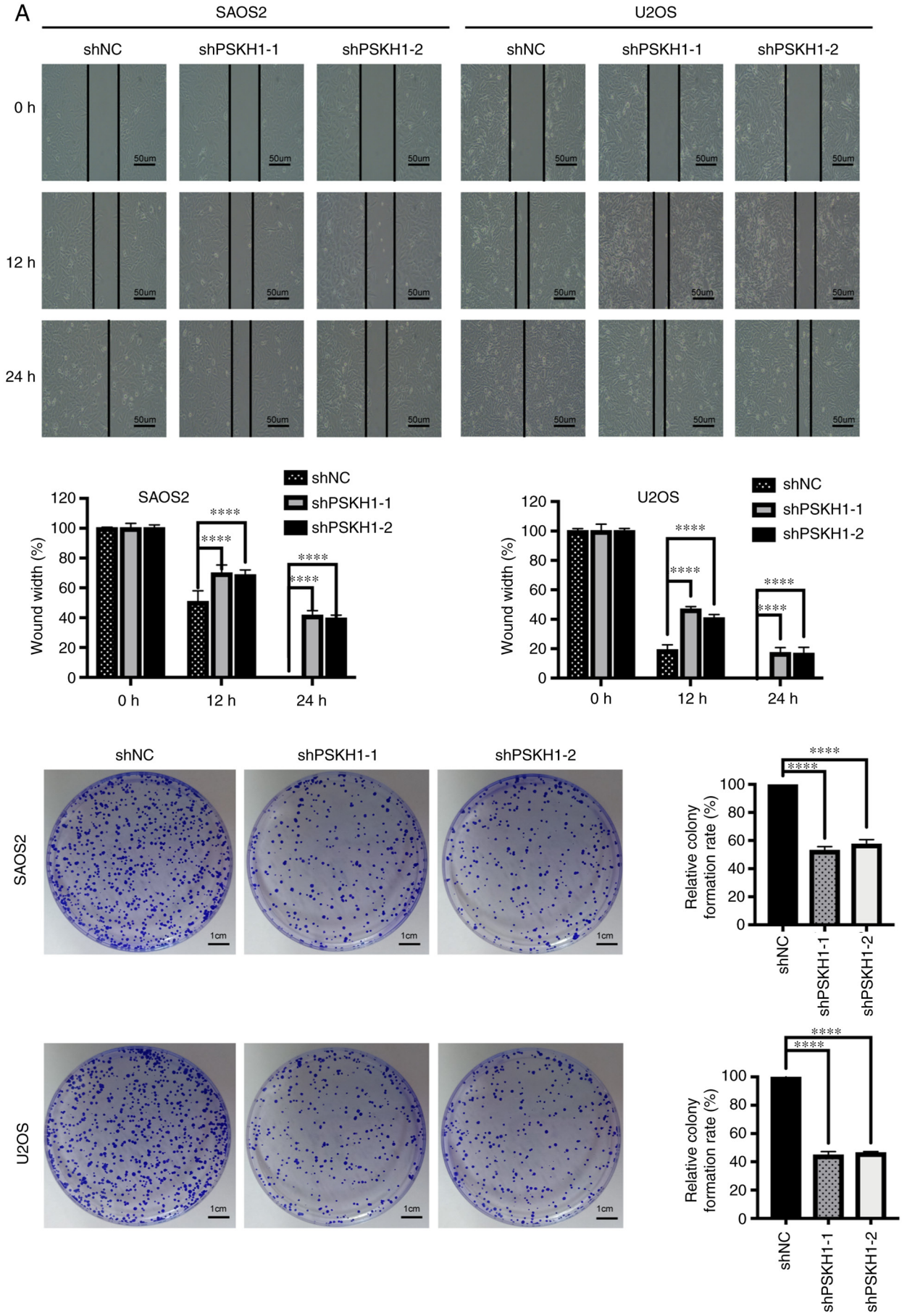

Figure 3. Effect of PSKH1 expression on wound healing and clonal expansion. (A) Wound healing in U2OS and SAOS2 cells transfected with lenti-shPSKH1 or lenti-shNC. Scale bar, 50 μm. (B) Clonal expansion of U2OS and SAOS2 cells transfected with lenti-shPSKH1 or lenti-shNC. Scale bar, 1 cm. PSKH1, protein serine kinase H1; sh, short hairpin; NC, negative control (****P<0.0001 vs. shNC).

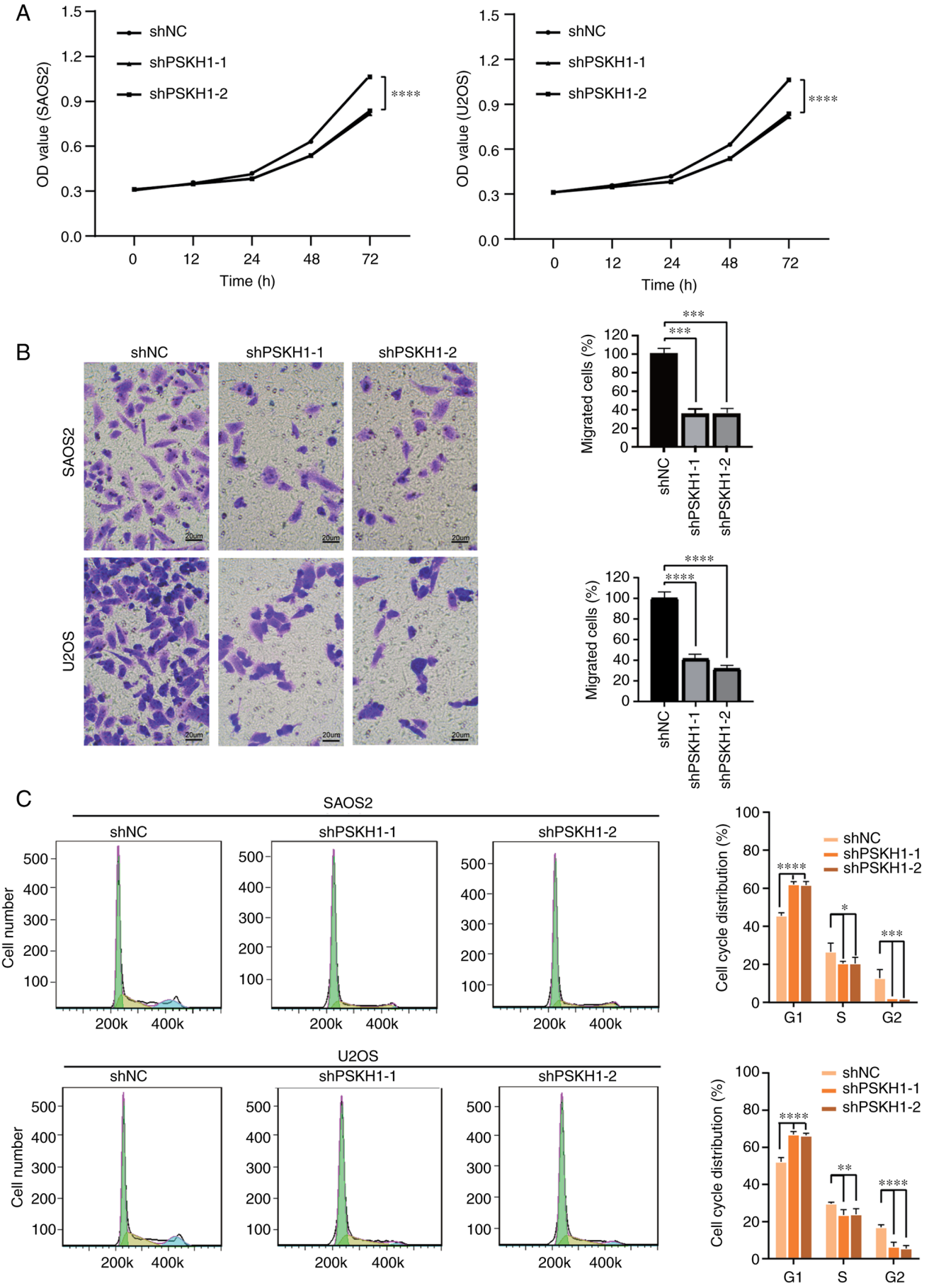

Figure 4. PSKH1 regulates proliferation, invasion and cell cycle in U2OS and SAOS2 cells. (A) Proliferation, (B) invasion and (C) cell cycle progression of U2OS and SAOS2 cells following transfection with lenti-shPSKH1 or lenti-shNC. Scale bar, 20 μm. PSKH1, protein serine kinase H1; sh, short hairpin; NC, negative control; OD, optical density (*P<0.05; **P<0.01; ***P<0.001; ****P<0.0001 vs. shNC).

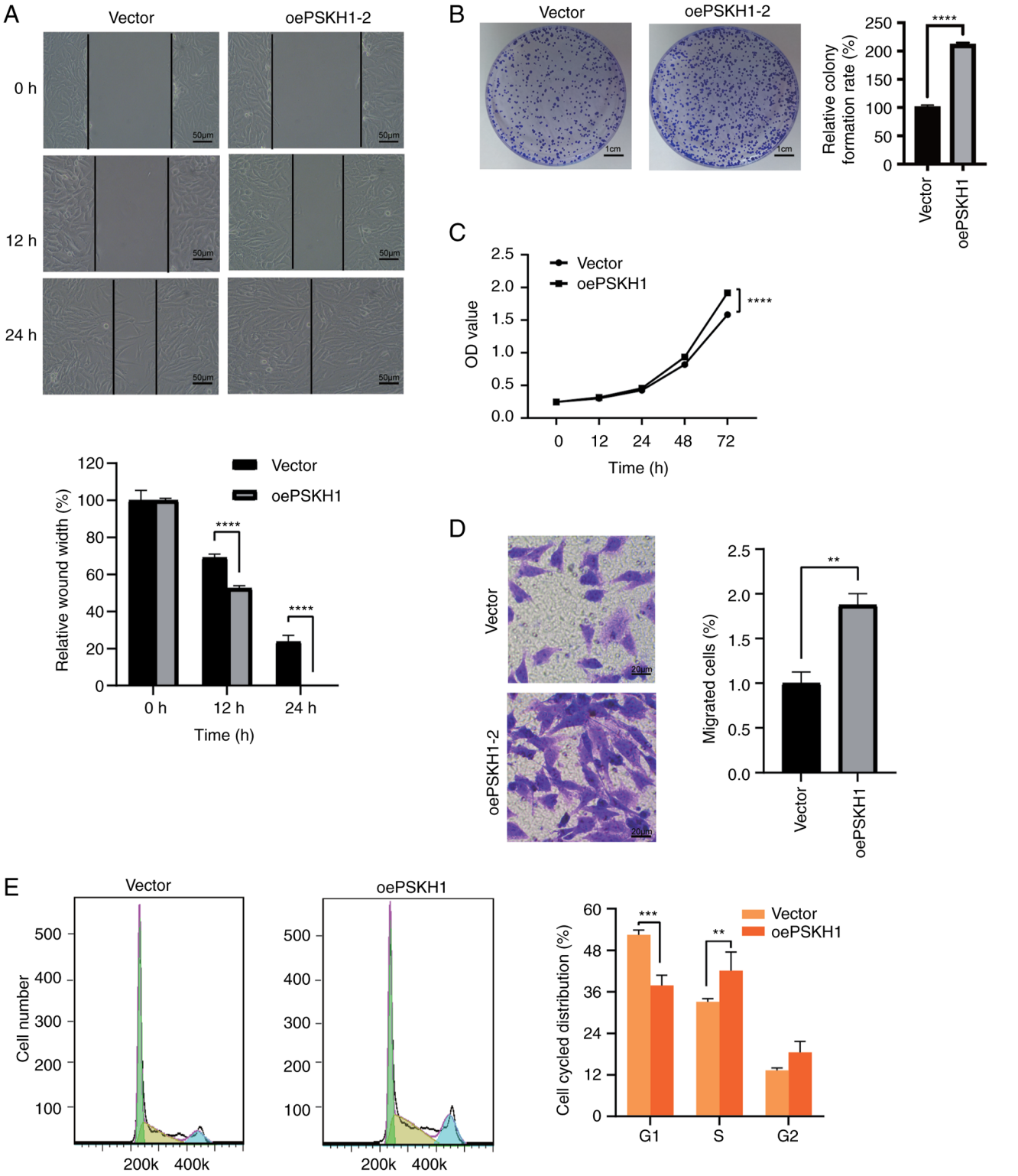

Figure 5. Effect of PSKH1 overexpression on MG63 cells. (A) Wound healing in MG63 cells with ectopic expression of PSKH1 and vector control. Scale bar, 50 μm. (B) Clonal expansion assay and (C) growth curve of MG63 cells, with ectopic expression of PSKH1 and vector control. Scale bar, 1 cm. (D) Invasion of MG63 cells with ectopic expression of PSKH1 and vector control. Scale bar, 20 um. (E) Cell cycle analysis in MG63 cells, with ectopic expression of PSKH1 and vector control. PSKH1, protein serine kinase H1; oe, overexpression; OD, optical density (**P<0.01; ***P<0.001; ****P<0.0001 vs. Vector).

PSKH1 serves an oncogenic role in OS cells via the p38 pathway. The potential mechanisms involved in OS pathogenesis were investigated. GSEA was conducted on OS and normal samples in the ArrayExpress database. PSKH1 expression was significantly associated with the p38 pathway (Fig. 7A). The p38 pathway regulates cell invasion and migration (20). To confirm GSEA results, the association between PSKH1, p38 and p-p38 was investigated *in vitro*. Overexpression of PSKH1 led to an elevation in the expression of p-p38 and an increase in the p-p38/p38 ratio in MG63

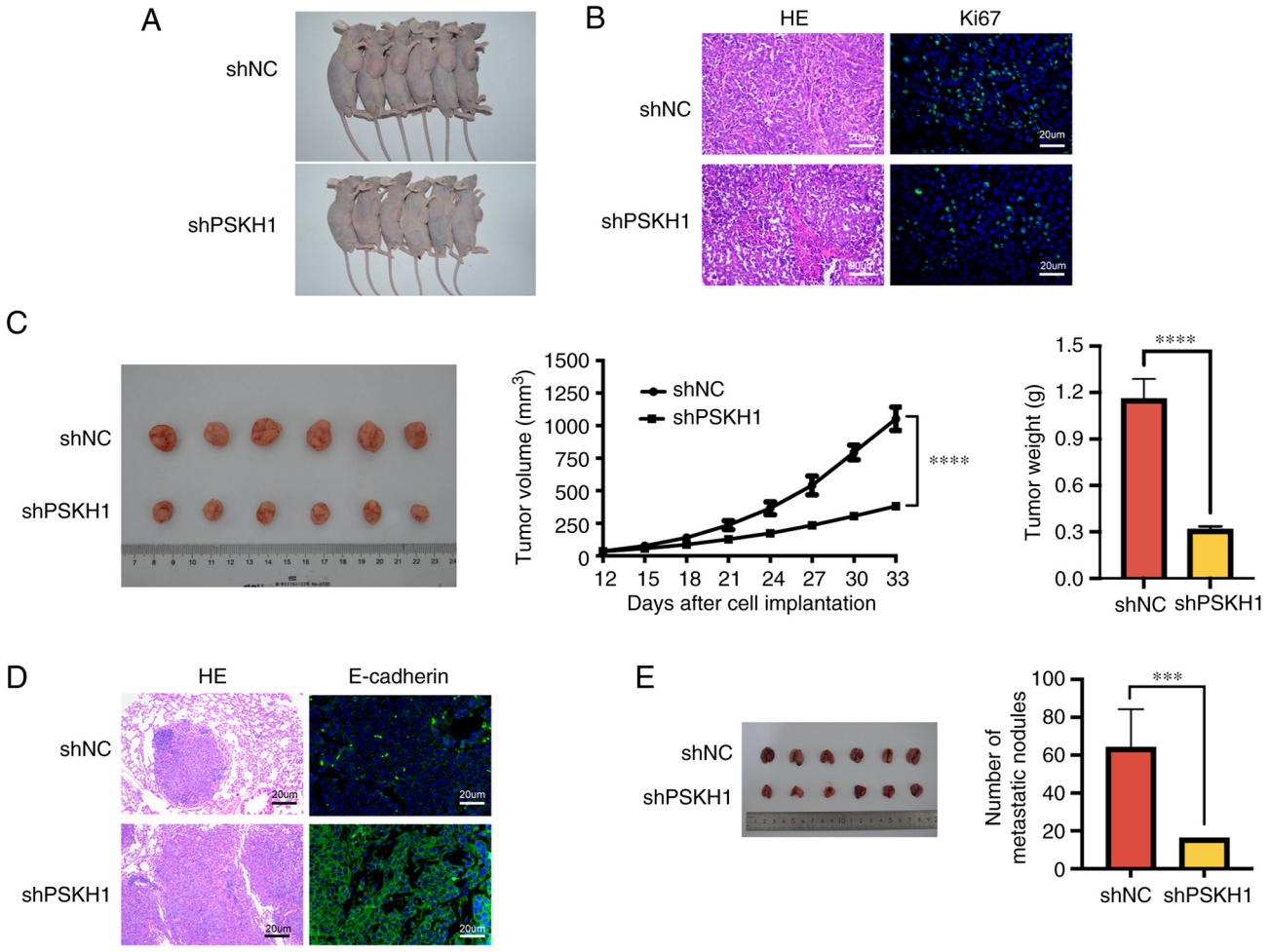

Figure 6. PSKH1 knockdown inhibits osteosarcoma growth and lung metastasis. (A) Xenograft subcutaneous tumors formed by shPSKH1 cells were smaller than those formed by shNC cells. (B) Immunofluorescence and HE staining of Ki67 expression. Scale bar, 20 um. (C) Tumor growth curve and weight (mean ± SD). (D) Immunofluorescence and HE staining of E-cadherin expression and lung metastatic nodules. Scale bar, 20 um. (E) Lung metastatic nodules were counted 8 weeks post-implantation. PSKH1, protein serine kinase H1; sh, short hairpin; NC, negative control; HE, hematoxylin and eosin (***P<0.001; ****P<0.0001 vs. shNC).

cells (Fig. 7B). Conversely, the silencing of PSKH1 through shPSKH1 resulted in a reduction of the expression of p-p38, resulting in a decrease in the ratio of p-p38/p38 in U2OS and SAOS2 cells (Fig. 7C). The effect of PSKH1 on proliferation, invasion and migration of OS cells via *the p38 pathway* was investigated *in vitro*. MG63 cells transfected with PSKH1 overexpression vector were treated with a p38 inhibitor, SB203580. The overexpression of PSKH1 had a noticeable impact in promoting the proliferation and migration of established osteosarcoma (OS) cells. However, the treatment with SB203580 effectively attenuated the migration and proliferation in comparison to the cells in the PSKH1 overexpression group (Fig. 7D and E). Additionally, PSKH1 overexpression also significantly increased the colony formation and invasion of OS cells, as well as the proportion of cells in the S phase. However, the treatment with SB203580 effectively reversed the cell cycle progression, invasion, and proliferation in comparison to the cells in the PSKH1 overexpression group (Fig. 8A-C). Furthermore, SB203580 also effectively restored the ratio of p-p38/p38 in established OS cells, which had been induced by the PSKH1 overexpression (Fig. 8D). Together, these results suggested that PSKH1 served an oncogenic role in the development of OS, potentially by activating the p38 pathway.

Discussion

The p38/MAPK-mediated signaling pathway is activated in many types of humoral tumor, including OS, and is implicated in the progression of tumors (17,36,37). MAPK is key for cell proliferation in gastric cancer (38,39). Cancer-associated fibroblast produces interleukin-32, which stimulates invasion and metastasis of breast cancer cells via integrin β3/p38/MAPK signaling (40,41).

In the present study, overexpression of PSKH1 significantly increased p-p38 expression. The p38 inhibitor SB203580 effectively rescued proliferation, migration, and invasion in PSKH1 overexpression OS cells. The present results were consistent with previous findings (42,43). The present study investigated the effect of PSKH1 in OS cell lines via phosphorylation of p38/MAPK. Further study is necessary to determine the effect of p38/MAPK signaling pathway *in vivo*. The present findings demonstrated that the p38/MAPK signaling pathway may be responsible for PSKH1 function in OS.

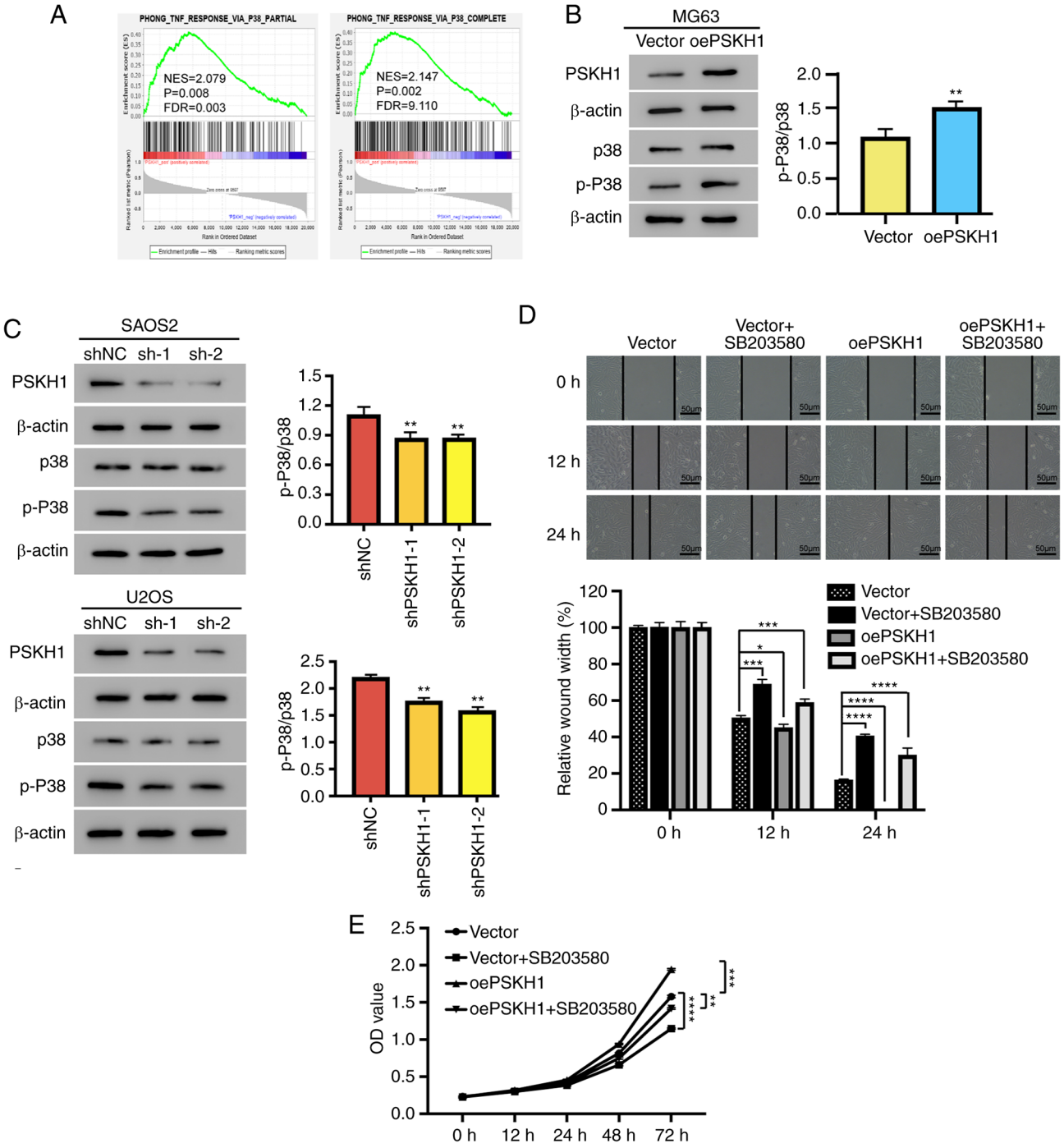

Figure 7. PSKH1 promotes OS cell proliferation by activating the p38 signaling pathway. The p38 pathway inhibitor SB203580 (10 μmol/l) was added to PSKH1-overexpressing OS cells and their controls for 24 h. (A) Association between PSKH1 expression and the p38-independent signaling pathway. (B) Protein expression of p-p38/p38 in MG63 cells with ectopic expression of PSKH1 and vector control (**P<0.01 vs. vector). (C) Protein expression of p-p38/p38 in U2OS and SAOS2 cells transfected with lenti-shPSKH1 or lenti-shNC. β-actin served as an internal control (**P<0.01 vs. shNC). (D) Wound healing in MG63 cells, with ectopic expression of PSKH1 after treatment with SB203580. Scale bar, 50 um (*P<0.05, ***P<0.001; ****P<0.0001 vs. vector). (E) Growth curve of MG63 cells with ectopic expression of PSKH1 and vector control after treatment with SB203580 (**P<0.01, ***P<0.001; ****P<0.0001 vs. vector). PSKH1, protein serine kinase H1; sh, short hairpin; NC, negative control; OS, osteosarcoma; p-, phosphorylated; OD, optical density; oe, overexpression; FDR, false discovery rate; NES, normalized enrichment score.

OS is a prevalent form of malignant bone tumor that primarily affects children and adolescents with a median age of 16 years (44). The tumor is commonly located in the long bones of the extremities, including the tibia, femur, and humerus. Despite the combination of traditional treatments, including wide resection, radiotherapy, and chemotherapy, providing a 5-year survival rate of 60 to 70% for non-metastatic OS patients (45), the prognosis for metastatic patients remains unfavorable with a high rate of recurrence and low survival rate of nearly 20% (46,47). Despite the efficacy of these treatments, the challenges of metastasis and relapse persist (48-50) and the underlying mechanisms of cell proliferation, migration, and invasion in OS remain elusive. Thus, identifying the molecular mechanisms underlying invasion and metastasis of OS cells

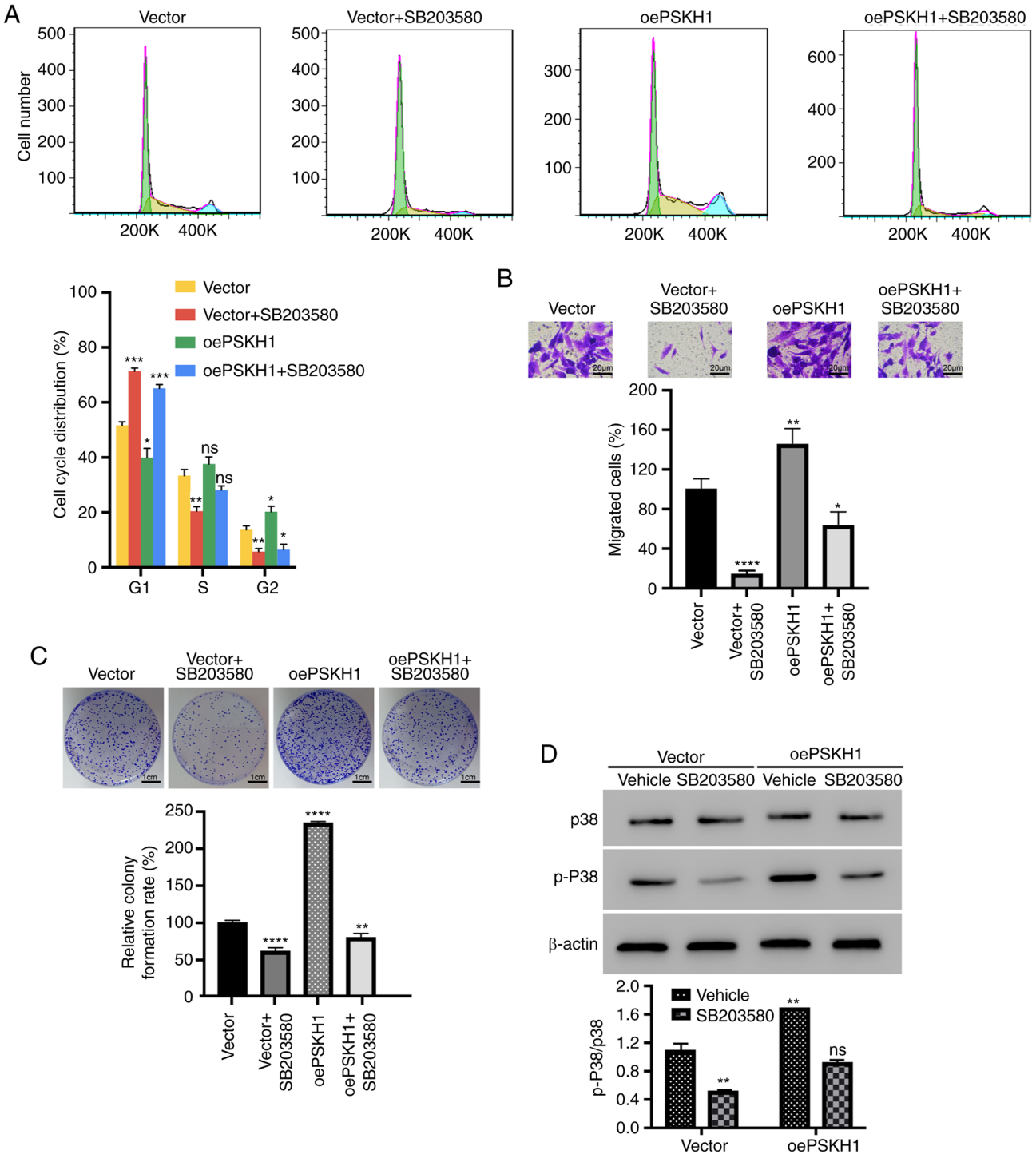

Figure 8. PSKH1 regulates the cell cycle via the p38 pathway. (A) Cell cycle analysis in MG63 cells with ectopic expression of PSKH1 and vector control following treatment with SB203580. (B) Migration of MG63 cells with ectopic expression of PSKH1 and vector control following treatment with SB203580. Scale bar, 20 um. (C) Clonal expansion assay of MG63 cells with ectopic expression of PSKH1 and vector control after treatment with SB203580. Scale bar, 1 cm. (D) Western blotting detected the protein expression of p-p38/p38 in MG63 cells with ectopic expression of PSKH1 and vector control following treatment with SB203580. PSKH1, protein serine kinase H1; p-, phosphorylated; oe, overexpression (*P<0.05, **P<0.01, ***P<0.001; ****P<0.0001 vs. vector).

may provide novel therapeutic targets. Previous studies have shown that PSKH1 is an autophosphorylating human protein involved in colon cancer (10,12). miR-566 directly targets PSKH1 and overexpression of PSKH1 reverses the biological effects of miR-566 (12). However, the role of PSKH1 in the proliferation, migration, and invasion of OS cells remains unresolved. The present findings demonstrated that PSKH1 may serve as a prognostic biomarker and a promising therapeutic target for OS. Gene expression profiling showed that high expression of PSKH1 in OS tissue was associated with poor prognosis. Furthermore, high levels of PSKH1 were detected in OS cell lines. The role of PSKH1 in OS cells was also investigated. Knockdown of PSKH1 suppressed OS cell proliferation, migration and invasion *in vitro*. The present

in vivo data support the role of PSKH1 in the development of OS. These findings are consistent with previous reports on colorectal cancer (10,12). The present findings indicated that PSKH1 may have an oncogenic role in the development of OS. A limitation of the present study was that the research was performed only in three OS cell lines. Future studies should investigate the role of PSKH1 and p38 in more OS cell lines, as well as other types of cancer.

In summary, the present data indicated that PSKH1 expression was associated with OS prognosis and PSKH1 may play an oncogenic role in OS via the p38/MAPK pathway. Therefore, PSKH1 may serve as a potential novel therapeutic target for OS.

Acknowledgements

Not applicable.

Funding

The present study was supported by the National Natural Science Foundation of China (grant nos. 81802721, 82001309) and Fundamental Research Funds for the Central Universities of China (grant no. 22120210570).

Availability of data and materials

The datasets used and/or analyzed during the current study are available from the corresponding author on reasonable request.

Authors' contributions

XFZ, YY and XZZ conceived and designed the study. XFZ, ZYW and YY performed the experiments; FY, ZYW and CJ analyzed and interpreted data. XFZ drafted the manuscript. XFZ and YY confirm the authenticity of all the raw data. All authors have read and approved the final manuscript.

Ethics approval and consent to participate

The study was approved (approval no. 2020-DW-007) by the Ethics Committee for Animal Experiments of Tongji Hospital, Shanghai, China. Animals were handled according to The Guide for the Care and Use of Laboratory Animals.

Patient consent for publication

Not applicable.

Competing interests

The authors declare that they have no competing interests.

References

1. American Cancer Society: Cancer Facts & Figures 2020. Am Cancer Soc: 1-52, 2020.
2. Meltzer PS and Helman LJ: New horizons in the treatment of osteosarcoma. N Engl J Med 385: 2066-2076, 2021.
3. Corre I, Verrecchia F, Crenn V, Redini F and Trichet V: The osteosarcoma microenvironment: A complex but targetable ecosystem. Cells 9: 976, 2020.
4. Gill J and Gorlick R: Advancing therapy for osteosarcoma. Nat Rev Clin Oncol 18: 609-624, 2021.
5. Belayneh R, Fourman MS, Bhogal S and Weiss KR: Update on osteosarcoma. Curr Oncol Rep 23: 71, 2021.
6. Shoaib Z, Fan TM and Irudayaraj JMK: Osteosarcoma mechanobiology and therapeutic targets. Br J Pharmacol 179: 201-217, 2022.
7. Sheng G, Gao Y, Yang Y and Wu H: Osteosarcoma and metastasis. Front Oncol 11: 780264, 2021.
8. Brede G, Solheim J and Prydz H: PSKH1, a novel splice factor compartment-associated serine kinase. Nucleic Acids Res 30: 5301-5309, 2002.
9. Brede G, Solheim J, Tröen G and Prydz H: Characterization of PSKH1, a novel human protein serine kinase with centrosomal, golgi, and nuclear localization. Genomics 70: 82-92, 2000.
10. Kim ST, Ahn TJ, Lee E, Do IG, Lee SJ, Park SH, Park JO, Park YS, Lim HY, Kang WK, *et al*: Exploratory biomarker analysis for treatment response in KRAS wild type metastatic colorectal cancer patients who received cetuximab plus irinotecan. BMC Cancer 15: 747, 2015.
11. Whitworth H, Bhadel S, Ivey M, Conaway M, Spencer A, Hernan R, Holemon H and Gioeli D: Identification of kinases regulating prostate cancer cell growth using an RNAi phenotypic screen. PLoS One 7: e38950, 2012.
12. Zhang Y, Zhang S, Yin J and Xu R: MiR-566 mediates cell migration and invasion in colon cancer cells by direct targeting of PSKH1. Cancer Cell Int 19: 333, 2019.
13. Yu H, Zou D, Ni N, Zhang S, Zhang Q and Yang L: Overexpression of NCAPG in ovarian cancer is associated with ovarian cancer proliferation and apoptosis via p38 MAPK signaling pathway. J Ovarian Res 15: 98, 2022.
14. Liu M, Zhou J, Liu X, Feng Y, Yang W, Wu F, Cheung OK, Sun H, Zeng X, Tang W, *et al*: Targeting monocyte-intrinsic enhancer reprogramming improves immunotherapy efficacy in hepatocellular carcinoma. Gut 69: 365-379, 2020.
15. Puri PL, Wu Z, Zhang P, Wood LD, Bhakta KS, Han J, Feramisco JR, Karin M and Wang JY: Induction of terminal differentiation by constitutive activation of p38 MAP kinase in human rhabdomyosarcoma cells. Genes Dev 14: 574-584, 2000.
16. Yu-Lee LY, Yu G, Lee YC, Lin SC, Pan J, Pan T, Yu KJ, Liu B, Creighton CJ, Rodriguez-Canales J, *et al*: Osteoblast-secreted factors mediate dormancy of metastatic prostate cancer in the bone via activation of the TGFβRIII-p38MAPK-pS249/T252RB pathway. Cancer Res 78: 2911-2924, 2018.
17. Wagner EF and Nebreda AR: Signal integration by JNK and p38 MAPK pathways in cancer development. Nat Rev Cancer 9: 537-549, 2009.
18. Comes F, Matrone A, Lastella P, Nico B, Susca FC, Bagnulo R, Ingravallo G, Modica S, Lo Sasso G, Moschetta A, *et al*: A novel cell type-specific role of p38alpha in the control of autophagy and cell death in colorectal cancer cells. Cell Death Differ 14: 693-702, 2007.
19. Igea A and Nebreda AR: The stress kinase p38α as a target for cancer therapy. Cancer Res 75: 3997-4002, 2015.
20. Kumar VB, Lin SH, Mahalakshmi B, Lo YS, Lin CC, Chuang YC, Hsieh MJ and Chen MK: Sodium danshensu inhibits oral cancer cell migration and invasion by modulating p38 signaling pathway. Front Endocrinol (Lausanne) 11: 568436, 2020.
21. Gerdes J, Li L, Schlueter C, Duchrow M, Wohlenberg C, Gerlach C, Stahmer I, Kloth S, Brandt E and Flad HD: Immunobiochemical and molecular biologic characterization of the cell proliferation-associated nuclear antigen that is defined by monoclonal antibody Ki-67. Am J Pathol 138: 867-873, 1991.
22. Gerdes J, Lemke H, Baisch H, Wacker HH, Schwab U and Stein H: Cell cycle analysis of a cell proliferation-associated human nuclear antigen defined by the monoclonal antibody Ki-67. J Immunol 133: 1710-1715, 1984.
23. Rioux-Leclercq N, Turlin B, Bansard J, Patard J, Manunta A, Moulinoux JP, Guillé F, Ramée MP and Lobel B: Value of immunohistochemical Ki-67 and p53 determinations as predictive factors of outcome in renal cell carcinoma. Urology 55: 501-505, 2000.
24. Krishna OH, Kayla G, Abdul Aleem M, Malleboyina R and Reddy Kota R: Immunohistochemical expression of Ki67 and p53 in wilms tumor and its relationship with tumor histology and stage at presentation. Patholog Res Int 2016: 6123951, 2016.
25. Dudderidge TJ, Stoeber K, Loddo M, Atkinson G, Fanshawe T, Griffiths DF and Williams GH: Mcm2, Geminin, and KI67 define proliferative state and are prognostic markers in renal cell carcinoma. Clin Cancer Res 11: 2510-2517, 2005.

26. Shi W, Hu J, Zhu S, Shen X, Zhang X, Yang C, Gao H and Zhang H: Expression of MTA2 and Ki-67 in hepatocellular carcinoma and their correlation with prognosis. Int J Clin Exp Pathol 8: 13083-13089, 2015.
27. Kankuri M, Söderström KO, Pelliniemi TT, Vahlberg T, Pyrhönen S and Salminen E: The association of immunoreactive p53 and Ki-67 with T-stage, grade, occurrence of metastases and survival in renal cell carcinoma. Anticancer Res 26: 3825-3833, 2006.
28. Zeng M, Zhou J, Wen L, Zhu Y, Luo Y and Wang W: The relationship between the expression of Ki-67 and the prognosis of osteosarcoma. BMC Cancer 21: 210, 2021.
29. Love MI, Huber W and Anders S: Moderated estimation of fold change and dispersion for RNA-seq data with DESeq2. Genome Biol 15: 550, 2014.
30. Subramanian A, Tamayo P, Mootha VK, Mukherjee S, Ebert BL, Gillette MA, Paulovich A, Pomeroy SL, Golub TR, Lander ES and Mesirov JP: Gene set enrichment analysis: A knowledge-based approach for interpreting genome-wide expression profiles. Proc Natl Acad Sci USA 102: 15545-15550, 2005.
31. Livak KJ and Schmittgen TD: Analysis of relative gene expression data using real-time quantitative PCR and the 2(-Delta Delta C(T)) method. Methods 25: 402-408, 2001.
32. Evangelisti C, Paganelli F, Giuntini G, Mattioli E, Cappellini A, Ramazzotti G, Faenza I, Maltarello MC, Martelli AM, Scotlandi K, *et al*: Lamin A and Prelamin A counteract migration of osteosarcoma cells. Cells 9: 774, 2020.
33. Niu G, Ye T, Qin L, Bourbon PM, Chang C, Zhao S, Li Y, Zhou L, Cui P, Rabinovitz I, *et al*: Orphan nuclear receptor TR3/Nur77 improves wound healing by upregulating the expression of integrin β4. FASEB J 29: 131-140, 2015.
34. Shi B, Xue M, Wang Y, Wang Y, Li D, Zhao X and Li X: An improved method for increasing the efficiency of gene transfection and transduction. Int J Physiol Pathophysiol Pharmacol 10: 95-104, 2018.
35. Xiang B, Geng R, Zhang Z, Ji X, Zou J, Chen L and Liu J: Identification of the effect and mechanism of Yiyi Fuzi Baijiang powder against colorectal cancer using network pharmacology and experimental validation. Front Pharmacol 13: 929836, 2022.
36. Shi D, Wu F, Mu S, Hu B, Zhong B, Gao F, Qing X, Liu J, Zhang Z and Shao Z: LncRNA AFAP1-AS1 promotes tumorigenesis and epithelial-mesenchymal transition of osteosarcoma through RhoC/ROCK1/p38MAPK/Twist1 signaling pathway. J Exp Clin Cancer Res 38: 375, 2019.
37. Fan MK, Zhang GC, Chen W, Qi LL, Xie MF, Zhang YY, Wang L and Zhang Q: Siglec-15 promotes tumor progression in osteosarcoma via DUSP1/MAPK pathway. Front Oncol 11: 710689, 2021.
38. Xia Y, Khoi PN, Yoon HJ, Lian S, Joo YE, Chay KO, Kim KK and Jung YD: Piperine inhibits IL-1β-induced IL-6 expression by suppressing p38 MAPK and STAT3 activation in gastric cancer cells. Mol Cell Biochem 398: 147-156, 2015.
39. Niu J, Yan T, Guo W, Wang W, Zhao Z, Ren T, Huang Y, Zhang H, Yu Y and Liang X: Identification of potential therapeutic targets and immune cell infiltration characteristics in osteosarcoma using bioinformatics strategy. Front Oncol 10: 1628, 2020.
40. Wen S, Hou Y, Fu L, Xi L, Yang D, Zhao M, Qin Y, Sun K, Teng Y and Liu M: Cancer-associated fibroblast (CAF)-derived IL32 promotes breast cancer cell invasion and metastasis via integrin β3-p38 MAPK signalling. Cancer Lett 442: 320-332, 2019.
41. Ni S, Li J, Qiu S, Xie Y, Gong K and Duan Y: KIF21B expression in osteosarcoma and its regulatory effect on osteosarcoma cell proliferation and apoptosis through the PI3K/AKT pathway. Front Oncol 10: 606765, 2021.
42. Jiang QG, Xiong CF and Lv YX: Kin17 facilitates thyroid cancer cell proliferation, migration, and invasion by activating p38 MAPK signaling pathway. Mol Cell Biochem 476: 727-739, 2021.
43. Fang Y, Yang J, Zu G, Cong C, Liu S, Xue F, Ma S, Liu J, Sun Y and Sun M: Junctional adhesion molecule-like protein promotes tumor progression and metastasis via p38 signaling pathway in gastric cancer. Front Oncol 11: 565676, 2021.
44. Siegel RL, Miller KD and Jemal A: Cancer statistics, 2018. CA Cancer J Clin 68: 7-30, 2018.
45. Anderson ME: Update on survival in osteosarcoma. Orthop Clin North Am 47: 283-292, 2016.
46. Saraf AJ, Fenger JM and Roberts RD: Osteosarcoma: Accelerating progress makes for a hopeful future. Front Oncol 8: 4, 2018.
47. Wang Z, Wang Z, Li B, Wang S, Chen T and Ye Z: Innate immune cells: A potential and promising cell population for treating osteosarcoma. Front Immunol 10: 1114, 2019.
48. Chen C, Xie L, Ren T, Huang Y, Xu J and Guo W: Immunotherapy for osteosarcoma: Fundamental mechanism, rationale, and recent breakthroughs. Cancer Lett 500: 1-10, 2021.
49. Whelan JS and Davis LE: Osteosarcoma, chondrosarcoma, and chordoma. J Clin Oncol 36: 188-193, 2018.
50. Gianferante DM, Mirabello L and Savage SA: Germline and somatic genetics of osteosarcoma-connecting aetiology, biology and therapy. Nat Rev Endocrinol 13: 480-491, 2017.